British Journal of Pharmacology (1997) 122, 379–385

Potent and voltage-dependent block by philanthotoxin-343 of neuronal nicotinic receptor/channels in PC12 cells

Min Liu, [1]Ken Nakazawa, Kazuhide Inoue & Yasuo Ohno

Division of Pharmacology, National Institute of Health Sciences, 1-18-1 Kamiyoga, Setagaya, Tokyo 158, Japan

1 Block by philanthotoxin-343 (PhTX-343), a neurotoxin from wasps, of ionic currents mediated through neuronal nicotinic acetylcholine (ACh) receptor/channels was characterized in rat phaeochromocytoma PC12 cells, by use of whole cell voltage-clamp techniques.

2 In the cells held at −60 mV, PhTX-343 at 0.1 and 1 μM inhibited an inward current activated by 100 μM ACh. The current inhibition was relieved by depolarizing steps, and augmented at negative potentials, suggesting that PhTX-343 blocks the channel in a voltage-dependent manner. Joro spider toxin-3 (JSTX-3) also exerted voltage-dependent inhibition of ACh-activated currents in a similar concentration range, but argiotoxin636 did not affect the currents.

3 Analysis of the current decay during hyperpolarizing steps indicated that the current inhibition by 100 nM PhTX-343 develops in an order of several hundreds of milliseconds. On the other hand, the recovery from the current inhibition during depolarizing steps developed in an order of about 100 ms.

4 The results suggest that PhTX-343 blocks neuronal nicotinic receptor channels in PC12 cells at concentrations lower than those required for channel block in non-mammalian cells, and the block exhibits clear voltage-dependence. Estimated from the voltage-dependence, the binding site of PhTX-343 may be located near the outer mouth of the channel.

Keywords: Philanthotoxin; Joro spider toxin; nicotinic acetylcholine receptors; ion channels; rat phaeochromocytoma

Introduction

The venoms of predatory wasps and spiders contain neurotoxins to paralyse insects (Clark *et al*., 1982; Abe *et al*., 1983; Jackson & Usherwood, 1988; Jackson & Parks, 1989). Such neurotoxins include substances that are potent blockers of ion channels. For spider toxins, low molecular weight toxins including Joro spider toxins (JSTX), toxins from New Guinea spider *Nephila maculata* (NSTX) and argiotoxin636 inhibit ionic currents through glutamate receptor/channels (see reviews, Jackson & Usherwood, 1988; Jackson & Parks, 1989) whereas ω-Aga-IVA, a peptide toxin from funnel web spider *Agelenopsis aperta*, selectively blocks ionic currents through P-type Ca^{2+} channels (Mintz *et al*., 1992). Philanthotoxins (PhTXs), low molecular weight toxins from wasps, have also been shown to affect both *N*-methyl-D-aspartate (NMDA) receptor/channels and nicotinic acetylcholine receptor/channels (Rozental *et al*., 1989; Anis *et al*., 1990). The inhibitory actions of PhTXs on these channels have mainly been deduced from the analysis of allosteric binding of the toxins. As for effects on channel functions, Rozental *et al*. (1989) have shown that the toxins inhibit ionic currents through nicotinic receptor/channels in frog muscle and cockroach thoracic ganglia at concentrations higher than 1 μM. No studies on the effects of PhTXs on mammalian neuronal type nicotinic receptor/channels have been published. Examination of the effects on these channels may be important because, when accidental injury by wasps occurs to man, the toxins may primarily affect peripheral perceptive neurones where nicotinic acetylcholine receptors play an essential role.

In the present study, we studied the effects of philanthotoxin-343 (PhTX-343) on ionic currents activated by acetylcholine in PC12 cells, an established mammalian neuronal cell line derived from a rat phaeochromocytoma (Greene & Tischler, 1976). In PC12 cells, neuronal type nicotinic receptors are expressed (Rogers *et al*., 1992), and the cells have been used to clarify the basic functional properties of these channels (Ifune & Steinbach, 1990; 1993). We found that PhTX-343 blocks nicotinic receptor/channels in these cells at concentrations lower than those required for the block of the channels in non-mammalian cells, and that the blocking action strongly depends on membrane potential.

Methods

PC12 cells (passage 55 to 70) were cultured according to Inoue & Kenimer (1988). We used undifferentiated PC12 cells because (1) it has been demonstrated that macroscopic currents permeating though nicotinic acetylcholine receptor/channels in these cells are large enough (usually > 100 pA at −60 mV) to study the effects of various compounds (Nakazawa *et al*., 1991b; 1994), and (2) although differentiation of these cells with nerve-growth factors (NGF) resulted in enlargement of the macroscopic currents (Nakazawa *et al*., 1991a) the NGF-treatment required longer culture periods (1 to 2 weeks) than untreated cells (2 to 5 days) until currents could be recorded. The cells were plated on collagen-coated coverslips and cultured in 35 mm polystyrene dishes. The coverslips were transferred into an experimental chamber of about 1 ml. Current recordings were made with conventional whole-cell voltage-clamp methods (Hamill *et al*., 1981) under the conditions described previously (Nakazawa *et al*., 1990; 1994). The cells were bathed in an extracellular solution containing (in mM): NaCl 140, KCl 5.4, $CaCl_2$ 1.8, $MgCl_2$ 1.0, HEPES 10, (+)-glucose 11.1 (pH was adjusted to 7.4 with NaOH). Tip resistances of heat-polished patch pipettes ranged between 3 to 5 MΩ when the pipettes were filled with an intracellular solution containing (in mM): CsCl 150, HEPES 10, ethyleneglycol-*bis*(2-aminoethylether)-N,N,N′,N′-tetraacetic acid (EGTA) 5 (pH 7.3 with CsOH). Application of ACh was made from an emitting tube (2 mm in inner diameter). Cells located near the mouth of the emitting tube (about 1 mm in distance) were selected for recordings, and the ACh-containing extracellular solution was applied rapidly (ca. 0.4 ml s^{-1}). To avoid desensitization of nicotinic receptor/channels, the period of each ACh application was brief (about 10 s), and each application

[1] Author for correspondence.

was separated by 3 min. Data were collected only from the cells which elicited reproducible inward currents with this application protocol. PhTX-343 and other toxins were applied for 10 to 20 s before and during the application of ACh. When voltage steps were applied, cells were stimulated repeatedly with a single type of voltage step (for example, a voltage step to +40 mV was applied for 400 ms every 3 s), and exposed to ACh. Thus, all the comparisons of the data obtained with different voltage protocols (e.g., +40 mV for 50 ms vs +40 mV for 100 ms) were made between different applications of ACh in this study. Experiments were performed at room temperature (about 25°C). Electrical signals were recorded with a patch clamp amplifier (Nihon Kohden CEZ-2400, Tokyo Japan), filtered at 5 kHz and stored on magnetic tape. Off-line analysis of membrane current was partly made by use of a software for patch/whole-cell clamp data (Nihon Kohden, QP-120J) on a personal computer (NEC PC9801RA2). Data were sampled at 1 kHz. Kinetics of the current were determined by plotting sampled data in a logarithmic manner, and time constants were calculated by the least squares methods programmed into the software.

Drugs used were: acetylcholine chloride (ACh; Wako), adenosine 5′-triphosphate disodium salt (ATP; Sigma), philanthotoxin-343 (PhTX-343; Tocris Cookson), Joro spider toxin-3 (JSTX-3; Wako) and argiotoxin636 (Latoxan).

Statistical analysis was made by Student;s *t* test. Differences were judged to be significant when $P<0.05$.

Results

Effects of PhTX-343 and other toxins on ACh-activated current

Figure 1a and b illustrates current traces obtained from PC12 cells. The cells were held at −60 mV and stepped to +10 mV for 400 ms every 3 s. ACh (100 μM) elicited an inward current at −60 mV, and this current was partially inhibited by 100 nM PhTX-343 (a) or JSTX-3 (b). The inhibition by PhTX-343 and JSTX-3 was dose-dependent: the EC_{50} was about 100 nM, and almost full inhibition was observed at 1 μM for both toxins (Figure 1c). On the other hand, argiotoxin636 (1 μM) inhibited only a small fraction (about 20%) of the ACh-activated current. After washout of the toxins, the inhibited currents recovered to 70 to 90% of the currents before the application of the toxins. In the presence of PhTX-343 or JSTX-3, the inward current at −60 mV was transiently enhanced after the depolarizing steps to +10 mV (Figure 1a and b). In other words, the depolarizing step appeared to recover the current fraction inhibited by the toxins. This phenomenon was further investigated in the following section (Figure 3).

The current inhibition by 100 μM PhTX-343 was not affected by the concentration of ACh used (Figure 2). The magnitude of the inhibition was comparable when the current was activated by either 30 or 300 μM ACh (Figure 2b).

Voltage-dependence of the current inhibition

Figure 3a illustrates a current trace obtained in the presence of 100 μM ACh and 100 nM PhTx-343. Application of a depolarizing step to +40 mV enhanced the inward current (the increased current fraction was indicated with a bar with arrows), as has been shown in Figure 1. It was assumed that this enhancement was due to attenuation of the inhibition by PhTX-343 because PhTX-343, as well as JSTX-3, is positively charged and thus its binding may be attenuated at positive potentials. In accord with this assumption, the current enhancement was more remarkable with a step to +40 mV than with a step to 0 mV (Figure 3b).

The idea of attenuation of the current inhibition at positive potentials predicts the facilitation of the current inhibition at negative potentials. This was confirmed by

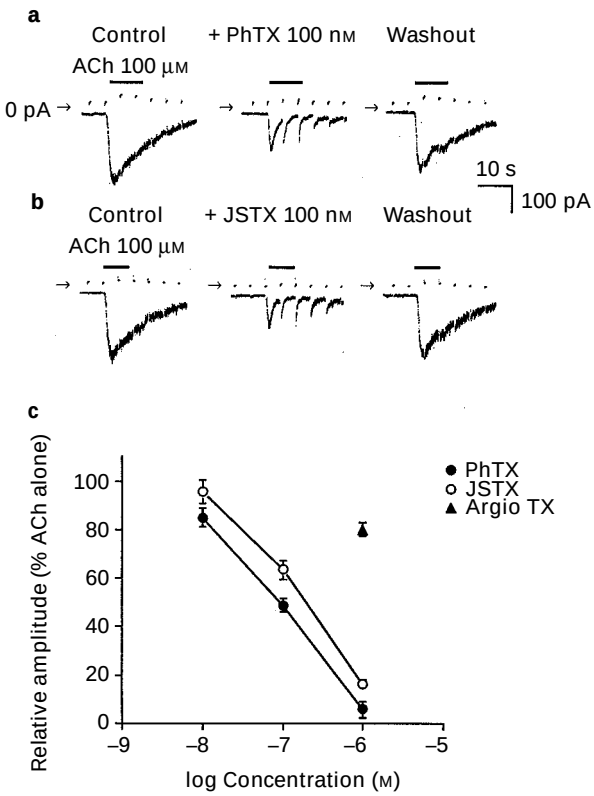

Figure 1 (a,b) Effects of PhTX-343 (100 nM; a) and JSTX-3 (100 nM; b) on ionic currents activated by 100 μM ACh. PC12 cells were held at −60 mV, and a 400 ms depolarizing voltage-step of +10 mV was applied every 3 s. ACh was applied to cells in the absence (left) or presence of the toxins (middle). The ACh-activated current after washout of the toxins is also shown (right). (c) Concentration-response relationship for the inhibition of the ACh-activated current. The ACh-activated current was elicited as in (a) and (b), and the peak current amplitude in the presence of the toxins was normalized to that before the application of the toxins. Each symbol represents a mean value obtained from 4–6 cells treated with PhTX-343, JSTX-3 or argiotoxin636 (ArgioTX). Vertical lines show s.e.mean.

experiments with hyperpolarizing step pulses (Figure 4). When a hyperpolarizing pulse of −120 mV was applied from −40 mV in the presence of 100 μM ACh and 100 nM PhTX-343, the inward current was gradually decreased (Figure 4a, +PhTX 100 nM). It is noted that no such decrease was observed when ACh alone was applied (Figure 1a, control). The decrease was more remarkable with a hyperpolarizing step to −120 mV than with a step to −80 mV (Figure 4b). Figure 4c shows the logarithmic plot of the current decay during the hyperpolarizing step to −120 mV in Figure 4a against time. Assuming a single exponential, the time course of the current decay was fitted with a time constant (τ) of 368 ms in this case. Like the magnitude of the current inhibition (Figure 4b), the time course was faster with a more hyperpolarizing step, and τ was smaller with a step to −120 mV than with a step to −80 mV (Figure 4d).

The voltage-dependence of the current inhibition was further investigated by holding the cells at different potentials (Figure 5). PhTX-343 (100 nM) inhibited the current activated by 100 μM ACh more strongly when the cells were held at −80 mV than when they were held at −40 mV (Figure 5a,b). In addition to the difference in the magnitude of the inhibition, a marked difference was also found in the time course of the ACh-activated current. In the presence of 100 nM PhTX-343, the ACh-activated current decayed much faster at −80 mV than at −40 mV (Figure 5a). To quantitate this current decay, we measured the current amplitude 5 s after the peak ACh-activated current. As shown in Figure 5c, the current activated

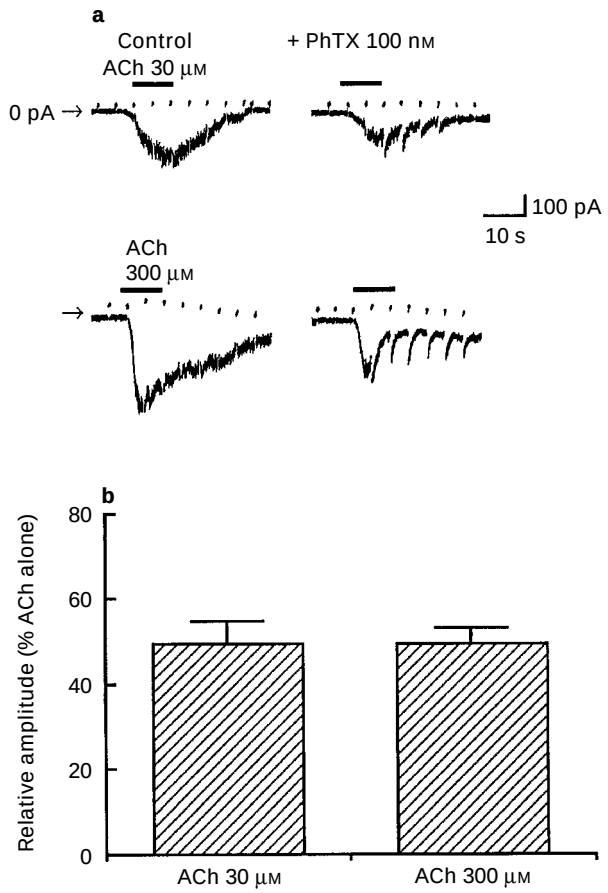

Figure 2 (a) Effects of PhTX-343 (100 nM) on ionic currents activated by 30 (upper traces) or 300 μM ACh (lower traces). Recordings were made as in Figure 1a. (b) Summarized data: the peak ACh-current in the presence of PhTX-343 (100 nM) was normalized to that before the application of the toxin in each cell. Data are mean $\pm$ s.e.mean from 5 cells.

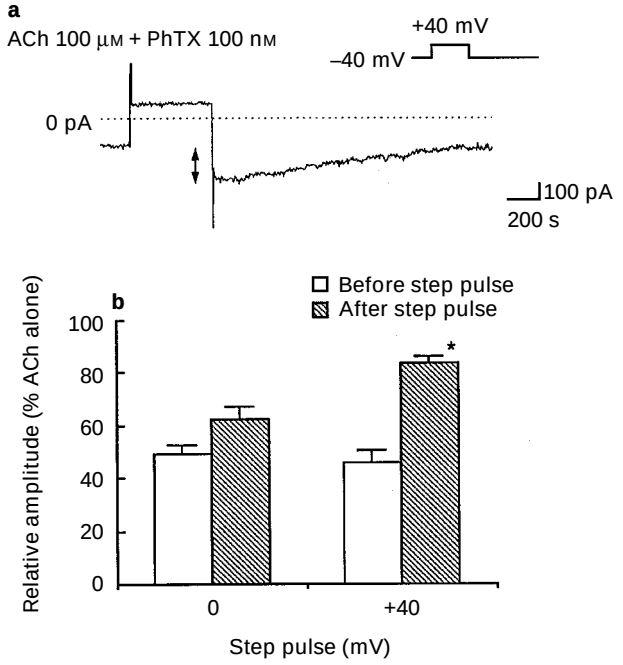

Figure 3 (a) Enhancement of ACh (100 μM)-activated current after the application of a depolarizing voltage step in the presence of 100 nM PhTX-343. The cell was held at -40 mV and stepped to $+40$ mV for 400 ms. The enhanced current at -40 mV was indicated by a bar with arrows. (b) Summarized data: the currents at -40 mV before and after the application of a depolarizing step in the presence of PhTX (100 nM) were normalized to those in the absence of the toxin. The cells were stepped to 0 (left or $+40$ mV (right), respectively. Data were obtained as in (a) from 5–6 cells. Vertical lines show s.e.mean. Asterisks indicate significant differences from the values before depolarizing steps ($P<0.05$).

by ACh alone decayed to about 80% of the peak amplitude in 5 s either at -40 or -80 mV. With 100 nM PhTX-343, the current decay was faster, and it was decreased to about 50% of the peak current in 5 s at -40 mV. The current decay was further accelerated at -80 mV and it was decreased to about 10% of the peak current in 5 s. Similar enhancement of the magnitude of the current inhibition (Figure 5b) and acceleration of the current decay at a more negative holding potential (Figure 5c) were also found with 100 nM JSTX.

The current inhibition by PhTX-343 was attenuated by depolarizing steps (Figures 1 and 3). To estimate how rapidly this attenuation occurs, depolarizing voltage steps of various durations were applied to cells. Figure 6a shows typical current traces obtained with the voltage steps. The currents after the voltage steps were gradually increased when the duration was prolonged from 20 to 50, then to 100 ms in this case. It was noted that an increase of outward currents was not observed during the depolarizing steps. This is because nicotinic receptor/channels exhibit strong inward rectification in PC12 cells (Ifune & Steinbach, 1990), and thus ACh does not produce marked outward currents at positive potentials. In all the cells tested, the inward current was maximally enhanced within 200 ms, and the time course could be fitted by a curve with a time constant of 60 ms (Figure 6b).

Lack of effect on ATP-activated current

ATP-activated channels (P2X purinoceptors) are abundantly expressed in PC12 cells (Nakazawa *et al.*, 1990). Effects of PhTX-343 and JSTX-3 on ATP-activated channels were tested. ATP (30 μM) elicited an inward current of 465 ± 71 pA at -60 mV (mean $\pm$ s.e.mean, $n=8$). PhTX-343 or JSTX-3 (100 nM) did not affect the ATP-activated current: the current amplitude in the presence of these toxins was 101.4 ± 2.0 (PhTX-343, $n=4$) or 101.2 ± 1.7 (JSTX-3, $n=4$) of control, respectively.

Discussion

PhTX-343 inhibited ionic currents mediated through nicotinic ACh receptor/channels in PC12 cells at submicromolar concentrations. It has been shown that PhTXs inhibit ionic currents mediated through nicotinic channels in frog muscle and cockroach thoracic ganglia, but the inhibition requires higher concentrations of PhTXs (higher than 1 μM: Rozental *et al.*, 1989). PC12 cells, a cell line derived from rat phaeochromocytoma, have been shown to express neuronal type nicotinic receptors: the receptors may consist of more than one population of heteropentameric receptors, where major constituents are $\alpha 3$ and $\beta 4$ subunits (Rogers *et al.*, 1992). The inhibition at submicromolar concentrations in the present study suggests that the receptors in PC12 cells may be more sensitive to PhTXs than the receptors in the insect ganglia and the amphibian muscle listed above. PhTXs have also been shown to act on NMDA receptors in a binding assay (Anis *et al.*, 1990) at micromolar concentrations or higher. The inhibition of the current through nicotinic receptor/channels at submicromolar concentrations was also found with JSTX-3. Inhibition by this toxin of nicotinic receptors has not been demonstrated. JSTX has been shown to inhibit glutamate receptor/channels at submicromolar concentrations (Abe *et al.*, 1983).

The current inhibition by PhTX-343 was voltage-dependent and it was augmented at negative potentials. Rozental *et al.* (1989) showed that PhTX blocked endplate currents in frog muscle and inward currents activated by iontophoretically applied ACh in cockroach neurones, and that the block was enhanced when cells were held at negative potentials. By superfusing ACh and applying voltage steps, the present study has further clarified the properties of the voltage-dependent block. The voltage-dependent inhibition is most readily explained by block at channel pores. The inhibition by positively charged blockers of nicotinic receptor channels such as hexamethonium is a classic example of pore blockade (Ascher *et al*, 1978). As PhTX-343, as well as JSTX-3, is also a positively charged compound (Nakanishi *et al.*, 1994) it may also block the pores of nicotinic receptor/channels. According to Woodhull (1973), this blockade can be regarded as a Bolzmann equilibrium distribution under a potential difference. Based on this theory, the equation that is available for estimation of voltage-dependence of the block is (Ravindran *et al.*, 1991; Nakazawa & Hess, 1993):

$$\ln\{(I_{max} - I)/I\} = \ln\{[B] + K_B(0)\} - \delta zEF/RT \qquad (1)$$

where I_{max} is current amplitude in the absence of toxins, [B] is the concentration of toxins, K_B is a dissociation constant, δ is the electrical distance from the outer mouth of the channel, z is a valence and E, F, R, and T are their general meanings. By use of the current fractions remaining after the inhibition at various potentials shown in Figures 3b, 4b and 5b, a plot was made according to equation (1) (Figure 7). The data for PhTX-343 shown in Figures 3b and 4b, where voltage steps were applied to examine voltage-dependence, can be fitted with a straight line with a slope of -0.019 mV^{-1}. On the other hand, the data for PhTX-343 shown in Figure 5b, which were obtained by changing holding potentials, slightly deviate from the line, presumably due to the different protocol used. From the slope of

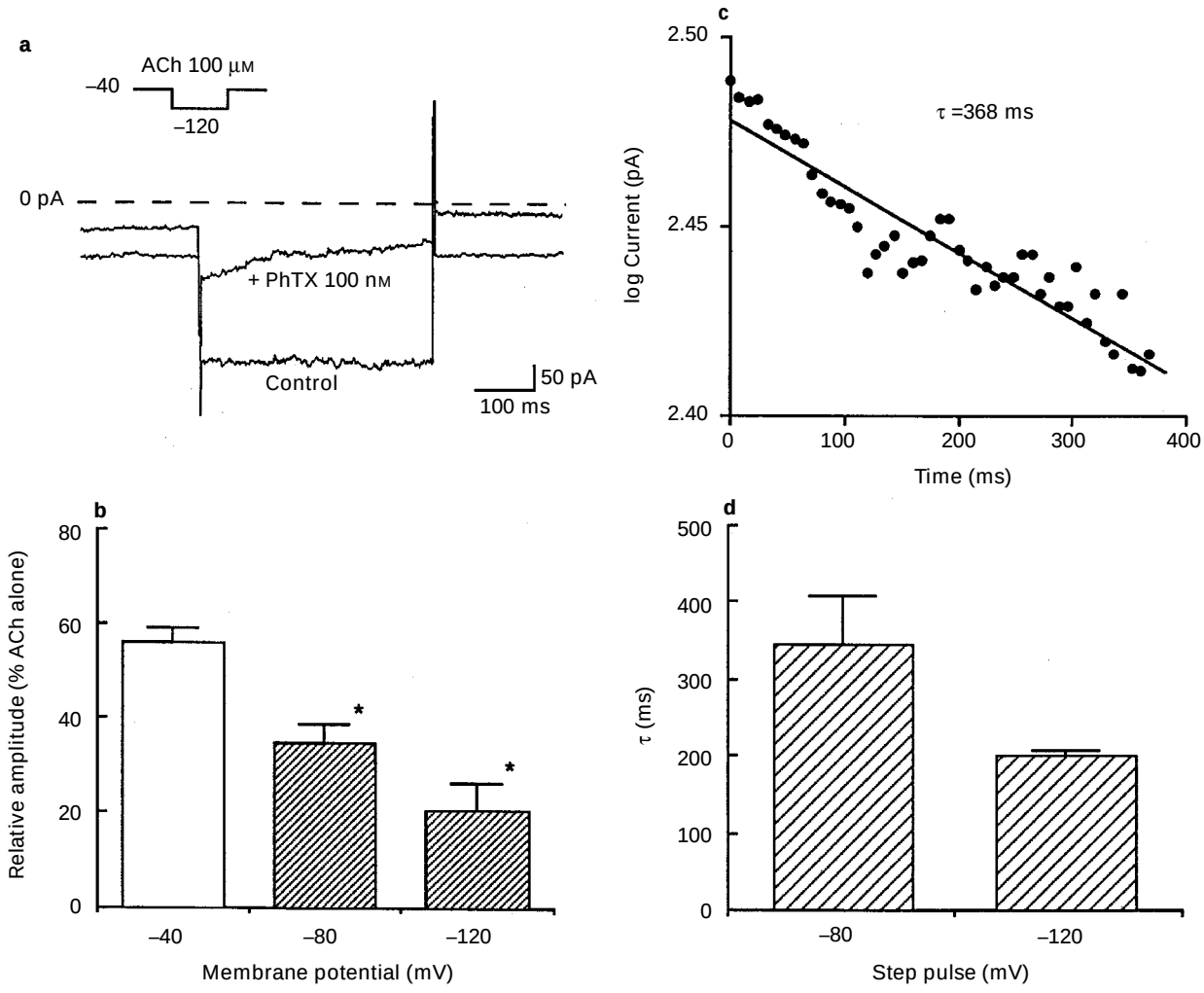

Figure 4 Changes in ACh-activated current in the presence of PhTX-343 when hyperpolarizing steps were applied. (a) Comparison of the current traces when a hyperpolarizing step of -120 mV was applied from a holding potential of -40 mV in the absence and presence of 100 nM PhTX-343. The inward current was elicited by 100 μM ACh. Note that the current at -120 mV decayed only in the presence of PhTX-343. (b) The current inhibition at different potentials. The cells were held at -40 mV and stepped to -80 or -120 mV as in (a). The amplitude of the current activation by ACh in the presence of PhTX-343 (100 nM) was normalized to that before the application of the toxin. The current at the holding potential of -40 mV (open column) and those at the test potentials of -80 and -120 mV (hatched columns) were compared. Data are mean$\pm$s.e.mean from 5–9 cells tested. Asterisks indicate significant differences from the values at -40 mV ($P<0.05$). (c) Time course of the current decay during hyperpolarization (-120 mV). The amplitude of the current with PhTX-343 shown in (a) was semilogarithmically plotted against time, and the data were fitted with a straight line assuming single exponential by use of the least square method. In this figure, only one-eighth of the data points used for the calculation are illustrated. (d) Summarized data for the time constant (τ) for the current decay during hyperpolarizing steps (-80 and -120 mV). τ was calculated as in (c). Data were mean$\pm$s.e.mean from 5–6 cells. No statistical difference was found between these two sets of data. Holding potential = -40 mV.

-0.019 mV^{-1} and assuming that PhTX-343 is a tricharged form ($z = +3$; Nakanishi *et al*., 1994), δ in equation (1) is calculated to be 0.16 (16% of total electrical distance). Thus, PhTX-343 may bind to a site rather close to the outer mouth of the channel.

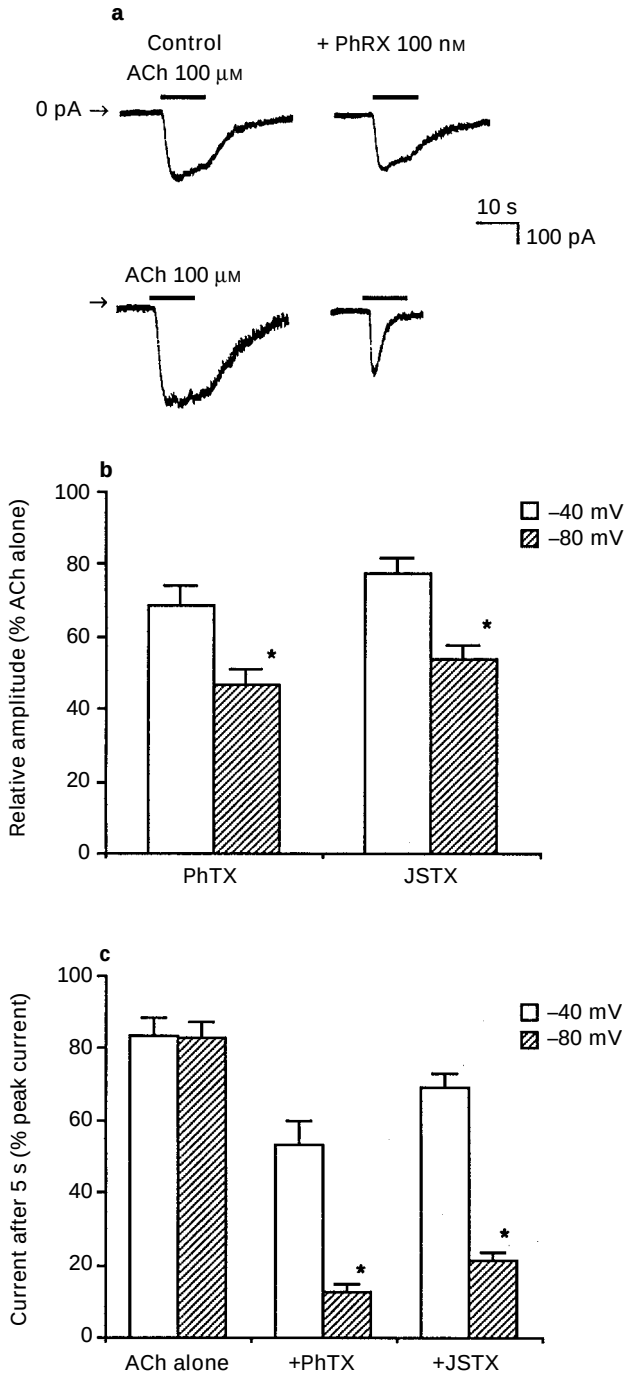

Figure 5 (a) Comparison of the inhibition by 100 nM PhTX-343 of ACh (100 μM)-activated current at different holding potentials. The ACh-activated current at -40 (upper traces) and that at -80 mV (lower traces) obtained in the absence (left) and presence of PhTX-343 (right) are shown. (b) Summarized data for the peak ACh-activated current. The current was recorded as in (a) with 100 nM PhTX-343 (left columns) or JSTX-3 (right columns). The current amplitude in the presence of the toxins was normalized to that before the application of the toxins. The data are mean $\pm$ s.e.mean from 5–7 cells tested. Asterisks indicate significant differences from the values at -40 mV ($P<0.05$). (c) Summarized data for the current remaining 5 s after the peak ACh-activated current. The current fraction remaining after 5 s was normalized to the peak amplitude. The data are mean $\pm$ s.e.mean from 5–7 cells tested. Asterisks indicate significant differences from the values at -40 mV ($P<0.05$).

If pore blockade is assumed, the following sequential model for channel behaviour can be applied for the inhibition by PhTX-343:

$$\underset{\text{(open)}}{A \cdot R + B} \underset{k_{-1}}{\overset{k_{+1}}{\rightleftharpoons}} \underset{\text{(blocked)}}{A \cdot R \cdot B} \quad \text{(scheme 1)}$$

where A is ACh, R is a nicotinic receptor/channel, B is PhTX-343, and k_{+1} and k_{-1} are rate constants. This scheme accounts for the enhancement of the decay of the ACh-activated current in the presence of PhTX-343 (Figure 5c) because transition to the blocked state (A.R.B) predicts the current decay. By introducing the reciprocal relation of τ and k_{+1}, k_{+1} was calculated to be 2.9 s^{-1} at -80 mV and 4.8 s^{-1} at -120 mV from the time course of the development of the inhibition upon hyperpolarization (Figure 4d). A dissociation rate constant, k_{-1}, was calculated to be 16.7 s^{-1} from the time course of the recovery from the inhibition observed with depolarizing prepulses (Figure 6b). Taking two relations, $k_{+1} = k'_{+1}$[PhTX-343] and $K_d = k_{-1}/k'_{+1}$, into account, K_d was calculated to be 580 nM for -80 mV or 350 nM for -120 mV. These values are somewhat larger than the IC_{50} of PhTX-343 at -60 mV (about 100 nM; Figure 1c). If the block occurs at the channel pore and PhTX-343 does not pass through the channel, k_{-1} re-

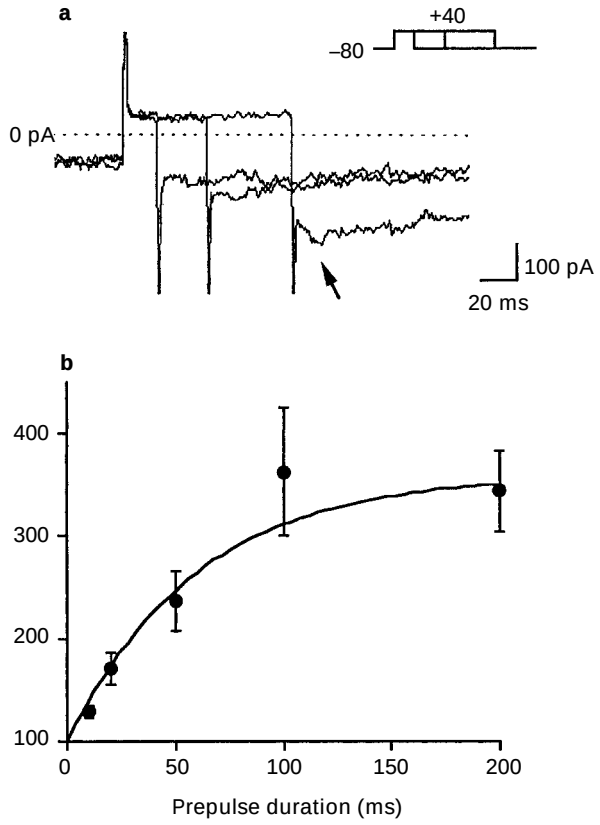

Figure 6 Attenuation of the current inhibition by PhTX-343 during depolarization. (a) Development of the recovery of the ACh-activated current during depolarization to $+40$ mV. The cell was held at -80 mV, and depolarizing steps of various durations were applied. ACh (100 μM) was applied in the presence of 100 nM PhTX-343. The current at -40 mV recovered after 100 ms depolarization, as indicated with an arrow. (b) Time course of the recovery during depolarization. ACh (100 μM) was applied in the presence of 100 nM PhTX-343 while cells were stimulated with depolarizing steps of various durations as in (a). Data are mean from 6 cells tested; vertical lines show s.e.mean. A curve was fitted to the data assuming a time constant (τ) of 60 ms.

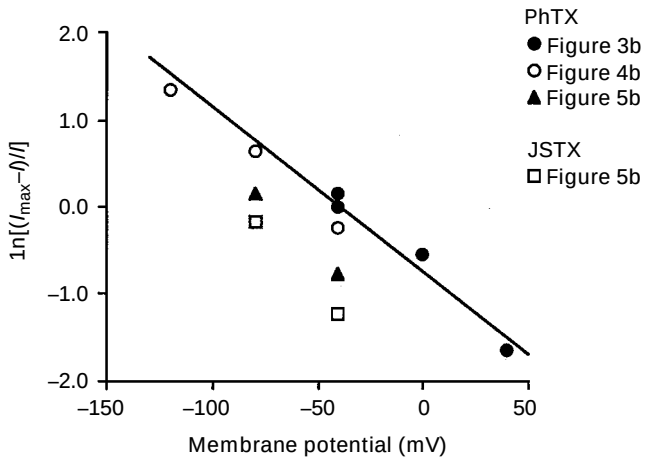

Figure 7 Analysis of voltage-dependence of the current inhibition to estimate the location of the binding site for PhTX-343. The data were plotted according to eq. (1) in the text. Symbols represent the mean values shown in Figure 3b, 4b and 5b for PhTX-343. The data for JSTX shown in Figure 5b were also plotted for comparison. The data were plotted against the membrane potential at which the current measurement was made with the exception of the data from Figure 4b which were plotted against prepulses, because these data represent the recovery during the prepulses. A straight line was drawn assuming a slope of $-0.019\ mV^{-1}$.

presents the rate constant for the escape of the toxin from the pore into the external solution. In this situation, k_{-1} would be smaller at negative potentials than at +40 mV, and, as a result, the calculated K_d will approach the measured value of 100 nM.

It is noted that our results cannot completely excluded explanations other than pore blockade. Competitive antagonism at the binding-site of ACh, at least, may not contribute to the current inhibition because the inhibition was not overcome by an increase in the concentration of ACh (Figure 2). On the other hand, an allosteric modulation could account for the current inhibition, as long as the modulation exhibits voltage-dependence.

Unlike nicotinic receptor/channels, ionic current mediated through ATP-activated channels was not affected by PhTX-343 or JSTX-3. The motif of ATP-activated channels has been shown to be completely different from those of other ligand-gated channels such as nicotinic or glutamate receptor/channels (Buell *et al*., 1996). The lack of effect of PhTX-343 or JSTX-3 indicates that the structure of the channel pore may be quite different between ATP-activated channels and nicotinic or glutamate receptor/channels, though all of these channels are non-selective cation channels.

As described above, the inhibition by PhTX-343 submicromolar concentrations appears peculiar to neuronal nicotinic receptors in PC12 cells. This channel inhibition may cause a marked influence on peripheral perceptive neurones when accidental injury by wasps occurs in man. In addition, the voltage-dependent nature of the inhibition may be relevant to detoxication: PhTX-343 may be readily removed from neuronal nicotinic channels under conditions where neurones are depolarized. The high-sensitivity of nicotinic receptor/channels to PhTX-343 and JSTX-3 shown in this study must be taken into account when this toxin is used as a pharmacological tool to distinguish the contribution of glutamatergic neurones to neurotransmission (Jackson & Usherwood, 1988; Jackson & Parks, 1989).

We are grateful to Ms T. Obama for culturing cells with her skilled techniques. M.L. is a visiting researcher supported by Japan China Medical Association.

References

ABE, T., KAWAI, N. & MIWA, A. (1983). Effects of a spider toxin on the glutaminergic synapse of lobster muscle. *J. Physiol.*, **339,** 243–252.

ANIS, N., SHERBY, S., GOODNOW, Jr, R., NIWA, M., KONNO, K., KALLIMOPOULOS, T., BUKOWNIK, R., NAKANISHI, K., USHERWOOD, P. ELDEFRAWI, A. & ELDEFRAWI, M. (1990). Structure-activity relationship of philanthotoxin analogs and polyamines on N-methyl-D-aspartate and nicotinic acetylcholine receptors. *J. Pharmacol. Exp. Ther.*, **254,** 764–113.

ASCHER, P., MARTY, A. & NEILD, T.O. (1978). Studies on the mechanism of action of acetylcholine antagonists on rat parasympathetic ganglion cells. *J. Physiol.*, **295,** 139–170.

BUELL, G., COLLO, G. & RASSENDREN, F. (1996). P2X receptors: an emerging channel family. *Eur. J. Neurosci.*, **8,** 2221–2228.

CLARK, R.B., DONALDSON, P.L., GRATION, K.A.F., LAMBERT, J.J., PIEK, T., RAMSEY, R., SPANJER, W. & USHERWOOD, P.N.R. (1982). Block of locust muscle glutamate receptors by δ-philanthotoxin occurs after receptor activations. *Brain Res.*, **241,** 105–114.

GREENE, L.A. & TISCHLER, A.S. (1976). Establishment of a noradrenergic clonal line of rat adrenal pheochromocytoma cell which respond to nerve growth factor. *Proc. Natl. Acad. Sci. U.S.A.*, **73,** 2424–2428.

HAMILL, O.P., MARTY, A., NEHER, E., SAKMANN, B. & SIGWORTH, F.J. (1981). Improved patch-clamp techniques for high-resolution current recordings from cells and cell-free membrane patches. *Pflügers Arch.*, **391,** 85–100.

IFUNE, C.K. & STEINBACH, J.H. (1990). Rectification of acetylcholine-elicited currents in PC12 pheochromocytoma cells. *Proc. Natl. Acad. Sci. U.S.A.*, **87,** 4794–4798.

IFUNE, C.K. & STEINBACH, J.H. (1993). Modulation of acetylcholine-elicited currents in clonal rat phaeochromocytoma (PC12) cells by internal polyphosphates. *J. Physiol.*, **463,** 431–447.

INOUE, K. & KENIMER, J.G. (1988). Muscarinic stimulation of calcium influx and norepinephrine release in PC12 cells. *J. Biol. Chem.*, **263,** 8157–8161.

JACKSON, H. & PARKS, T.N. (1989). Spider toxins: recent applications in neurobiology. *Ann. Rev. Neurosci.*, **12,** 405–414.

JACKSON, H. & USHERWOOD, P.N.R. (1988). Spider toxins as tools for dissecting elements of excitatory amino acid transmission. *Trends Neurosci.*, **11,** 278–283.

MINTZ, I.M., VENEMA, V.J., SWIDEREK, K.M., LEE, T.D., BEAN, B.P. & ADAMS, M.E. (1992). P-type calcium channels blocked by the spider toxin ω-Aga-IVA. *Nature*, **355,** 827–829.

NAKANISHI, K., CHOI, S.-K., HWANG, D., LERRO, K., ORLANDO, M., KALIVERETENOS, A.G., ELDEFRAWI, A., ELDEFRAWI, M. & USHERWOOD, P.N.R. (1994). Bioorganic studies of transmitter receptors with philanthotoxin analogs. *Pure Appl. Chem.*, **66,** 671–678.

NAKAZAWA, K., FUJIMORI, K., TAKANAKA, A. & INOUE, K. (1990). An ATP-activated conductance in pheochromocytoma cells and its suppression by extracellular calcium. *J. Physiol.*, **428,** 257–272.

NAKAZAWA, K., FUJIMORI, K., TAKANAKA, A. & INOUE, K. (1991a). Comparison of adenosine triphosphate- and nicotine-activated inward currents in pheochromocytoma cells. *J. Physiol.*, **434,** 647–660.

NAKAZAWA, K. & HESS, P. (1993). Block by calcium of ATP-activated channels in pheochromocytoma cells. *J. Gen. Physiol.*, **101,** 377–392.

NAKAZAWA, K., INOUE, K., KOIZUMI, S., IKEDA, M. & INOUE, E. (1994). Inhibitory effects of capsaicin on acetylcholine-evoked responses in rat phaeochromocytoma cells. *Br. J. Pharmacol.*, **113,** 296–302.

NAKAZAWA, K., WATANO, T., OHARA-IMAIZUMI, M., INOUE, K., FUJIMORI, K., OZAKI, Y., HARADA, M. & TAKANAKA, A. (1991b). Inhibition of ion channels by hirsutine in rat pheochromocytoma cells. *Jpn. J. Pharmacol.*, **57,** 507–515.

RAVINDRAN, A., SCHILD, L. & MOCZYDLOWSKI, E. (1991). Divalent cation selectivity for external block of voltage-dependent Na^+ channels prolonged by batrachotoxin. Zn^{2+} induces discrete substates in cardiac Na^+ channels. *J. Gen. Physiol.*, **97,** 98–115.

ROGERS, S.W., MANDELZYS, A., DENERIS, E.S., COOPER, E. & HEINEMANN, S. (1992). The expression of nicotinic acetylcholine receptors by PC12 cells treated with NGF. *J. Neurosci.*, **12,** 4611 – 4623.

ROZENTAL, R., SCOBLE, G.T., ALBUQUERQUE, E.X., IDRISS, M., SHERBY, S., SATTELLE, D.B., NAKANISHI, K., KONNO, K., ELDEFRAWI, A.T., ELDEFRAWI, M.E. (1989). Allosteric inhibition of nicotinic acetylcholine receptors of vertibrates and insects by philanthotoxin. *J. Pharmacol. Exp. Ther.*, **249,** 123 – 130.

WOODHULL, A.M. (1973). Ionic blockade of sodium channels in nerve. *J. Gen. Physiol.*, **61,** 687 – 708.

(Received March 20, 1997
Revised May 21, 1997
Accepted June 16, 1997)